Contract No. 582-23-45978
Work Order No. 12
Tracking No. 2025-11
Task 5.2

Prepared for:

Texas Commission on Environmental Quality
12100 Park 35 Circle MC 164
Austin, TX 78753

Prepared by:

Ramboll
7250 Redwood Blvd., Suite 105
Novato, California 94945

June 27, 2025

Fire Emissions Inventory Development for 2019 and 2023 Modeling and Evaluation

PREPARED UNDER A CONTRACT FROM THE
TEXAS COMMISSION ON ENVIRONMENTAL QUALITY

The preparation of this document was financed through a contract from the State of Texas through the Texas Commission on Environmental Quality.
The content, findings, opinions and conclusions are the work of the author(s) and do not necessarily represent findings, opinions or conclusions of the TCEQ.

RAMBOLL

Fire Emissions Inventory Development for 2019 and 2023 Modeling and Evaluation

Final Report

Ramboll
7250 Redwood Boulevard
Suite 105
Novato, CA 94945
USA

T +1 415 899 0700
https://ramboll.com

Contents

Table of Figures

Table of Tables

LIST OF ACRONYMS AND ABBREVIATIONS

3-D	Three-dimensional
ABI	Advanced Baseline Imager
ACM2	Asymmetric Convective Mixing, version 2
AQ	Air Quality
BC	Black Carbon
CAMx	Comprehensive Air quality Model with extensions
CAMS	Copernicus Atmospheric Monitoring Service
CAMS	Continuous Ambient Monitoring Stations
CB6r5	Carbon Bond version 6, Revision 5
CF2	Coarse/Fine 2-mode particulate matter chemistry
C-IFS	Composition Integrated Forecasting System
CMAQ	Community Multiscale Air Quality Model
CO	Carbon Monoxide
CST	Central Standard Time
EBI	Euler Backward Iterative solver
ECMWF	European Centre for Medium-Range Weather Forecasts
EPA	Environmental Protection Agency
FEER	Fire Energetics and Emissions Research
FEI	Fire Emission Inventory
FINN	Fire INventory from NCAR
FRP	Fire Radiative Power
GEOS	Goddard Earth Observing System
GEOS-Chem	Goddard Earth Observing System Chemical global model
GFAS	Global Fire Assimilation System
GOES	Geostationary Operational Environmental Satellite
HGB	Houston-Galveston-Brazoria
HRRR-Smoke	High Resolution Rapid Refresh model with smoke
IS4FIRES	Integrated monitoring and modelling System for wildland FIRES project
Ix	Inorganic Iodine
JPSS	Joint Polar Satellite System
kg	kilogram
km	kilometer
m	meter
MDA8	Maximum Daily Average 8-hour
MODIS	MODerate resolution Imaging SpectroRadiometer
MPE	Model Performance Evaluation
NCAR	National Center for Atmospheric Research
netCDF	network Common Data Format
NMB	Normalized mean bias
NME	Normalized mean error (unsigned, or gross)
NOx	Nitrogen oxides
NRT	Near-Real Time

OC	Organic Carbon
PBL	Planetary Boundary Layer
PBL500	Planetary Boundary Layer height plus 500 meters
PM	Particulate Matter
$PM_{2.5}$	Particulate Matter less than 2.5 microns
ppb	parts per billion
PPM	Piecewise Parabolic Method
QFED	Quick Fire Emissions Dataset
RAVE	Regional Advanced baseline imager and Visible infrared imaging radiometer suite fire Emissions
SIP	State Implementation Plan
TCEQ	Texas Commission on Environmental Quality
ug	microgram
US	United States
VIIRS	Visible Infrared Imaging Radiometer Suite
VOC	Volatile organic compounds
WRF	Weather Research and Forecasting model
WRF-Chem	Weather Research and Forecasting model with Chemistry

PROJECT SUMMARY

The TCEQ requires emission estimates of criteria pollutants and key precursors from fires across the continental United States and parts of Canada, Mexico, Central America, and the Caribbean for State Implementation Plan (SIP) modeling. This project developed and evaluated various fire emissions estimates for 2019 and 2023, then recommended which processed inventories are best suited for TCEQ's modeling needs.

EXECUTIVE SUMMARY

The TCEQ has previously utilized the Fire Inventory from the National Center for Atmospheric Research version 2.2 (FINN2.2) for State Implementation Plan (SIP) modeling. Previous project work (Ramboll, 2023) evaluated ozone model performance for TCEQ's 2019 modeling platform and suggested that the use of FINN v2.2 contributed to ozone overestimates when transport of smoke from biomass burning in Mexico and Central America was frequent. Ramboll (2023) found that the Global Fire Assimilation System version 1.2 (GFAS1.2) fire emissions inventory (FEI) showed substantially smaller modeled ozone biases and overall better statistical agreement with observations compared to FINN. All modeling was conducted using the Comprehensive Air quality Model with extensions (CAMx; Ramboll, 2024b).

Like other FEIs, GFAS1.2 has daily temporal and 0.1° spatial resolution. A newer FEI, Regional Hourly Advanced Baseline Imager (ABI) and Visible Infrared Imaging Radiometer Suite (VIIRS) Emissions version 2.0 (RAVE2.0), offers finer temporal (hourly) and spatial (0.03°) resolution. Ramboll (2024a) found RAVE2.0 resulted in the best overall model agreement with ozone and $PM_{2.5}$ observations among all available FEIs in a CAMx application for the active Summer 2021 wildfire season in the Western U.S. Since RAVE2.0 fire emissions are only available from 2021 onward, we developed GFAS1.2 fire emissions for the April-September 2019 CAMx modeling application and developed both GFAS1.2 and RAVE2.0 emissions for the 2023 application. Both years used TCEQ's modeling platforms. We could not perform CAMx modeling and evaluation for 2022 because TCEQ's 2022 modeling platform was not ready in time for this project.

Our evaluation of the 2019 GFAS1.2 CAMx simulation shows good ozone performance across all regions, with lower monthly bias and error than TCEQ's 2019 modeling, which used FINN2.2 fire emissions. This result aligns with our more extensive testing of four different FEIs for the shorter April-May 2019 period (Ramboll, 2023). The ozone evaluation for the 2023 CAMx simulations found similar results between GFAS1.2 and RAVE2.0. GFAS1.2 exhibited slightly better performance during April-May, while RAVE2.0 performed slightly better during August-September, when observed ozone was highest. We recommend RAVE2.0 for 2023 due to its superior ozone performance during the highest ozone periods.

Ramboll recommends three activities to improve the FEI processor and support TCEQ's needs:

- Complete model performance evaluation for 2022 and provide recommendations for choice of FEI
- Use CAMx to evaluate FEI processor updates that use fire intensity rather than fuel type for VOC speciation
- Develop model-ready fire emissions for 2024 using multiple FEIs and conduct CAMx simulations and ozone and $PM_{2.5}$ evaluation

1.0 INTRODUCTION

1.1 Background

For State Implementation Plan (SIP) modeling, TCEQ requires emission estimates of criteria pollutants and important precursors from fires in the continental United States, as well as parts of Canada, Mexico, Central America, and the Caribbean that are encompassed in TCEQ's modeling domains. TCEQ has previously utilized the Fire Inventory from the National Center for Atmospheric Research version 2.2 (FINN2.2). Previous project work (Ramboll, 2023) evaluated ozone model performance for TCEQ's 2019 modeling platform and suggested that the use of FINN v2.2 contributed to ozone overestimates when transport of smoke from biomass burning in Mexico and Central America was frequent. Ramboll (2023) found that the Global Fire Assimilation System version 1.2 (GFAS1.2) fire emissions inventory (FEI) exhibited substantially smaller modeled ozone biases and overall better statistical agreement with observations compared to FINN. Like FINN2.2, GFAS1.2 has daily temporal and 0.1° spatial resolution. The other FEI of interest is the Regional Hourly Advanced Baseline Imager (ABI) and Visible Infrared Imaging Radiometer Suite (VIIRS) Emissions version 2.0 (RAVE2.0) dataset. The RAVE2.0 FEI combines fine temporal (hourly) and spatial (0.03°) resolution. Ramboll (2024a) found RAVE2.0 exhibited the best overall modeled agreement with ozone and $PM_{2.5}$ observations among all available FEIs for an application focused on the active Summer 2021 wildfire season in the Western U.S. However, RAVE does not provide fire emissions prior to 2021. This project provides fire emissions modeling inputs for 2019 (GFAS) and 2023 (GFAS and RAVE) and allows TCEQ to choose the FEI best suited for future photochemical modeling of ozone and $PM_{2.5}$.

1.2 Project Objectives

The purpose of this work is to develop and evaluate different fire emissions estimates and provide recommendations on which of the processed inventories is the most suitable for incorporating into TCEQ's 2023 modeling. Recommendations are based on the analysis of ozone and particulate matter (PM) results from model sensitivity runs over April to September of 2023 using the Comprehensive Air quality Model with extensions (CAMx; Ramboll, 2024b). These modeling results demonstrate the impact of FEI selection on modeling accuracy with regards to ozone production and particulate matter.

2.0 2019 AND 2023 FIRE EMISSIONS PROCESSING

The FEI processor was used to develop model inputs from raw FEI datasets for 2019 (GFAS) and 2023 (GFAS and RAVE) modeling years. Comprehensive details of the FEI processor and descriptions of the FEI datasets are discussed in previous reports (Ramboll, 2022; 2023; 2024a).

2.1 FEI Summary

The FEI processor was originally developed in 2022 and updated in each following year. It is currently designed to generate fire emissions inputs from the following five global FEI products:

- Fire Inventory from NCAR version 2.5 (FINN2.5)
- Global Fire Assimilation version 1.2 (GFAS1.2)
- Quick Fire Emissions Dataset version 2.4 (QFED2.5)
- Fire Energetics and Emissions Research version 1.0 (FEER1.0)
- Regional ABI and VIIRS fire Emissions version 2.0 (RAVE2.0)

Descriptions and key characteristics of each of the FEIs above are available in previous reports. Table 2-1 summarizes key characteristics of the two FEIs evaluated in this project.

Table 2-1. Summary of key characteristics of select FEIs.

FEI	Horizontal Resolution	Timeframe	Frequency	Approach	Burned Area/FRP Methodology	Emissions Species	Modeling Applications
RAVE2.0	3 x 3 km over North America	2021–Present	Hourly with 24-hour lag	FRP	GOES, VIIRS	NOx, total VOC, CO, SO2, NH3, OC, BC, $PM_{2.5}$	HRRR-Smoke; CMAQ; WRF-Chem
GFAS1.2	0.1°×0.1°	2003–present	Daily with 24-hour lag	FRP	MODIS	NOx, VOC, CO, SO2, NH3, OC, BC, $PM_{2.5}$	CAMS C-IFS

2.1.1 GFAS1.2

GFAS multiplies fire radiative power (FRP) reported from MODIS Aqua/Terra satellite measurements by landcover-specific conversion factors to obtain dry matter combustion rate estimates. GFAS then employs a sophisticated filtering system that masks spurious FRP signals from volcanoes, gas flaring and other industrial activity. GFAS includes vertical parameters – plume bottom, plume top and mean altitude of maximum injection height (described in Remy et al., 2017), all of which are derived from a plume rise model. GFAS also provides a separate injection height from IS4FIRES (Remy et al., 2017). As with the fire emissions, these vertical parameters have daily resolution which correspond to early afternoon. The European Centre for Medium-Range Forecasts (ECMWF) Composition Integrated Forecasting System (C-IFS) of Copernicus Atmospheric Monitoring Service (CAMS) utilizes GFAS1.2 for global real time fire and smoke forecasts. GFAS1.2 is available in near real-time at 0.1° resolution.

2.1.2 RAVE2.0

RAVE2.0 is available from 2021 onward and utilizes a new algorithm to generate hourly fire emissions at 0.03° (~3 km) spatial resolution by fusing temporally resolved GOES Advanced Baseline Imager (ABI) FRP and fine spatial-resolution (375 m) FRP from the Visible Infrared Imaging Radiometer Suite (VIIRS) on the Joint Polar Satellite System (JPSS) satellites (Li et al., 2022). RAVE2.0 is available as a near real-time product and a "re-processed" historical product that both cover North America. By

contrast, the RAVE1.0 near real-time product covered North America, but the re-processed historical product covered the continental U.S. only. Hourly emissions are produced from land cover and ecoregion-specific FRP diurnal cycles using 5-minute GOES ABI FRP measurements. RAVE's combination of high temporal and spatial resolution is unique and thus appears well-suited for high resolution photochemical modeling. We use the high resolution landcover and landcover-specific diurnal profiles developed by the RAVE team for all non-RAVE FEIs, including GFAS1.2. RAVE2.0 emissions contain optional "scaled" emission species for primary $PM_{2.5}$, organic carbon (OC), and black carbon (BC), which the RAVE team developed for NOAA forecasting applications[1]. These scaled emissions are higher than the equivalent aerosol emission species as provided in the RAVE1.0 product and CAMx evaluations have revealed large $PM_{2.5}$ overestimations at monitoring locations resulting from using these scaled emissions. We therefore used the unscaled $PM_{2.5}$ emissions for the 2023 modeling period.

2.2 FEI Processor Overview

Figure 2-1 presents an overview of the FEI processor. Each of the FEI processing steps (regridding, chemical species mapping, temporal allocation and vertical plume rise) are shown in the blue hatched box. Ramboll (2023) details each of these steps. The FEI processor provides output gridded emissions in CAMx-ready 3-D netCDF format.

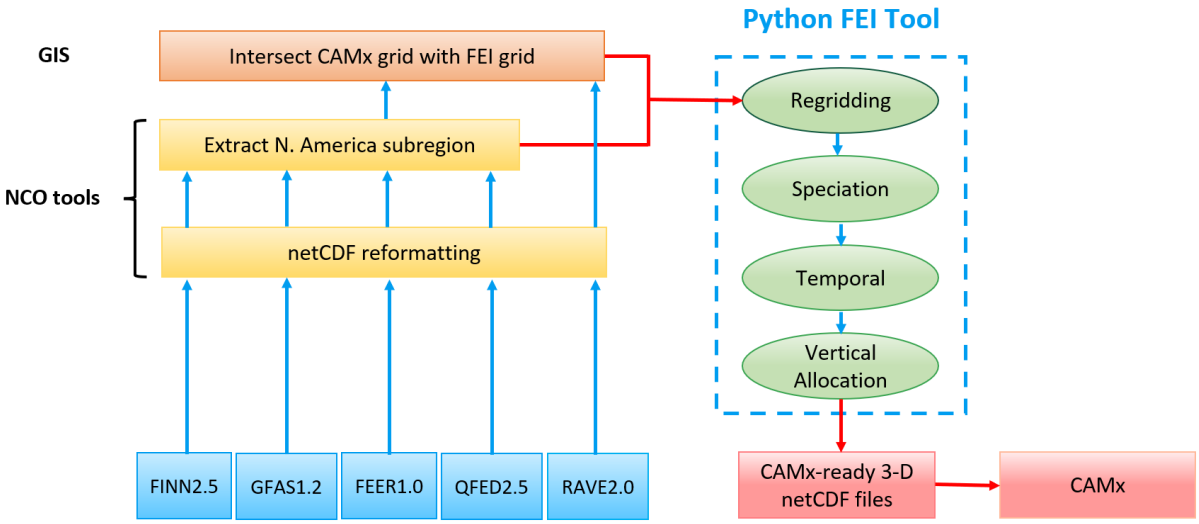

Figure 2-1. Flow diagram for processing gridded FEIs.

2.3 Fire Emission Summary Comparison

Figure 2-2 presents the spatial distribution of 2019 annual NOx (top left), $PM_{2.5}$ (top right) and VOC (bottom) GFAS fire emissions over the TCEQ 36 km CAMx domain. Figure 2-3 shows similar maps for 2023 RAVE (left) and GFAS (right) emissions. Relative to 2019, the 2023 GFAS totals are generally higher, particularly across Canada, Mexico, and regions of the central and southeastern United States. Despite these differences in magnitude, the spatial distribution patterns between 2019 and 2023 GFAS emissions remain broadly consistent. A comparison between the 2023 RAVE and GFAS inventories (Figure 2-3) shows that RAVE estimates are higher than GFAS.

[1] Personal communication, Fangjun Li

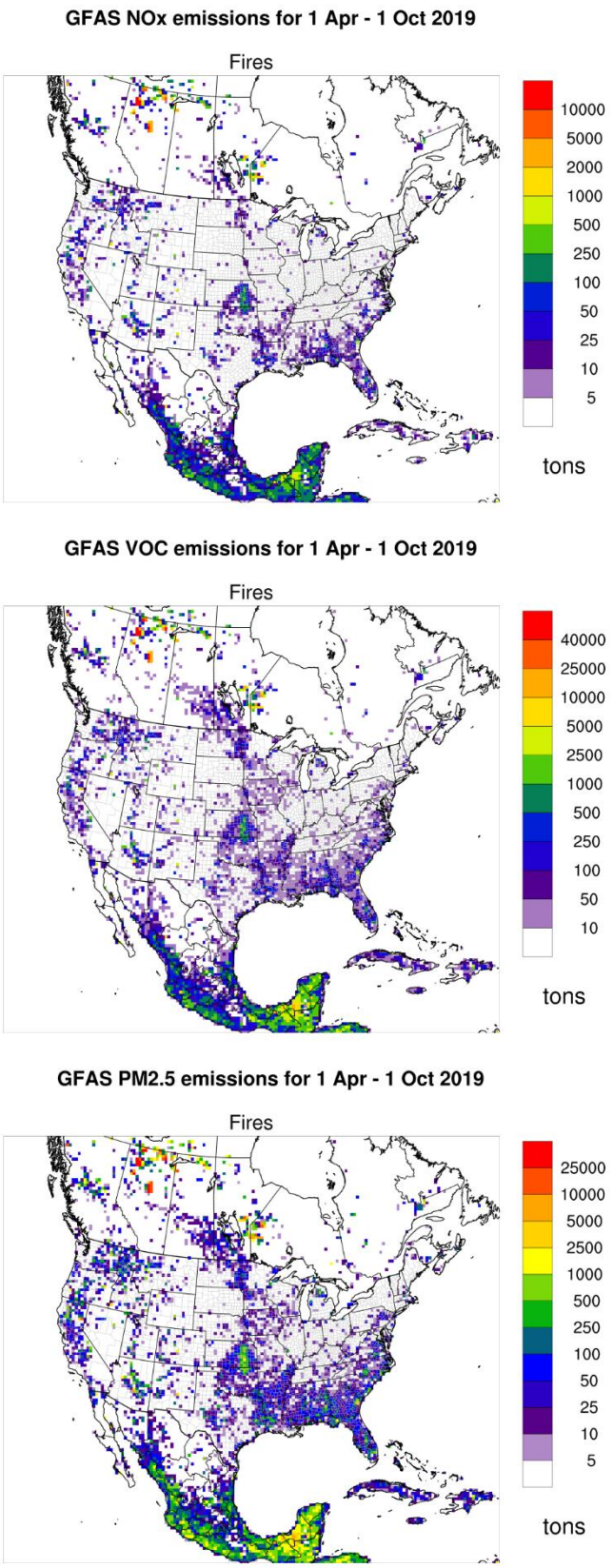

Figure 2-2. April-September 2019 NOx (top), VOC (middle) and $PM_{2.5}$ (bottom) fire emissions from GFAS1.2 over the TCEQ 36 km CAMx domain.

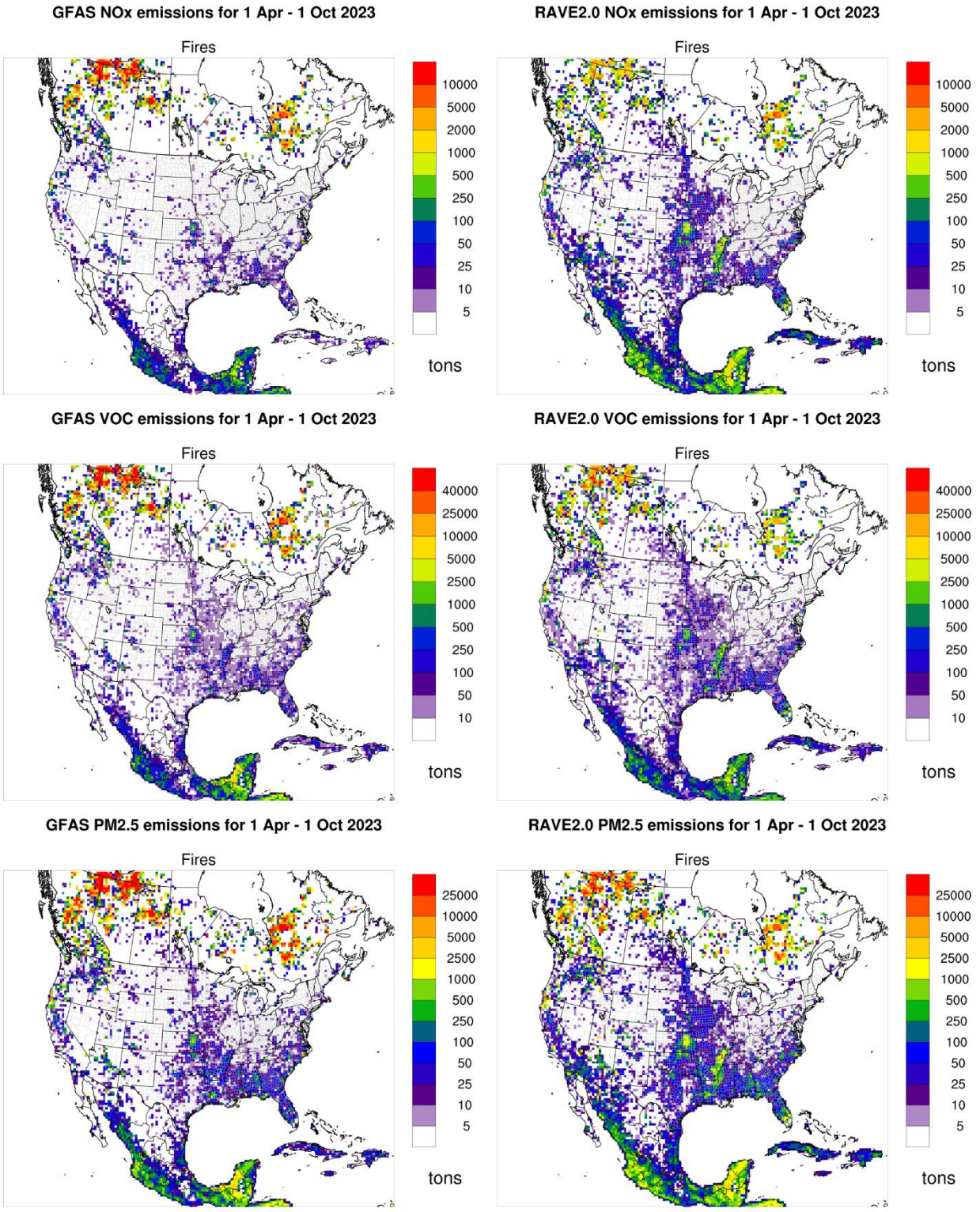

Figure 2-3. April-September 2023 NOx (top row), VOC (middle row), and $PM_{2.5}$ (bottom row) fire emissions for RAVE2.0 (left column) and GFAS1.2 (right column) over the TCEQ 36 km CAMx domain.

Table 2-2 lists the comparison of emissions estimates across the three inventories processed for this project: 2019 GFAS, 2023 GFAS, and 2023 RAVE. Estimates are summed across the Contiguous United States, Mexico, Central America and Texas. For the Contiguous U.S., emissions from the 2023 GFAS inventory show moderate increases over 2019 GFAS across all pollutants. The 2023 RAVE inventory reports substantially higher emissions, particularly for $PM_{2.5}$ and CO, with values nearly double those in 2023 GFAS. Within Texas, 2023 GFAS emissions are slightly lower than 2019 GFAS with ~11-16 % decrease across all the pollutants. 2023 RAVE emissions show larger estimates compared to 2023 GFAS — most prominently for NO_x (about 206% higher), and $PM_{2.5}$ (about 78% higher). Within Mexico and Central America, the 2023 RAVE emission estimates are higher than the 2023 GFAS emissions for CO, NOx and $PM_{2.5}$. However, 2023 RAVE VOC emissions are 40-50% lower than the 2023 GFAS VOC emissions.

Table 2-2. Emission summaries of 2019 GFAS1.2, 2023 GFAS1.2, and 2023 RAVE2.0 for Contiguous U.S, Mexico, Central America and Texas regions.

Regions/2019 GFAS1.2	**CO**	**NOx**	**VOC**	**$PM_{2.5}$**
Contiguous U.S.	2,187,804	52,797	281,417	211,335
Mexico	4,830,771	97,630	739,100	437,641
Central America	990,380	16,496	175,377	88,859
Texas	142,311	3,535	17,533	12,722
Regions/2023 GFAS1.2	**CO**	**NOx**	**VOC**	**$PM_{2.5}$**
Contiguous U.S.	2,381,552	56,896	308,435	246,582
Mexico	3,781,320	75,434	584,844	344,072
Central America	1,208,226	20,121	213,808	108,309
Texas	123,168	3,034	15,535	10,643
Regions/2023 RAVE2.0	**CO**	**NOx**	**VOC**	**$PM_{2.5}$**
Contiguous U.S.	4,400,821	165,169	448,721	440,232
Mexico	5,315,535	201,675	345,309	428,709
Central America	1,622,976	55,938	100,574	124,513
Texas	204,423	9,285	18,015	18,936

3.0 MODEL PERFORMANCE EVALUATION FOR 2019 AND 2023

The CAMx simulations were conducted for April-September of 2019 and 2023 utilizing TCEQ's CAMx modeling platforms. CAMx simulations for the year 2019 were conducted using the GFAS1.2 fire emissions inventory, as the RAVE2.0 Fire Emissions Inventory (FEI) was not available prior to 2021. For 2023, simulations were performed using both GFAS1.2 and RAVE2.0 FEI datasets to facilitate comparative analysis of fire emission impacts. While no CAMx modeling was performed for 2022 as part of this analysis, fire emission inventories from both GFAS1.2 and RAVE2.0 were developed for that year and delivered to TCEQ for integration into their 2022 modeling applications. This section provides a comprehensive evaluation of model performance for simulated ozone and particulate matter (PM) concentrations during the 2019 and 2023 modeling periods.

3.1 Model configuration

Model simulations for 2019 and 2023 were conducted for the April to September period (with 16-day spin-up period spanning March 16-31) using a two-way nested grid system consisting of a North American domain at 36 km resolution, a U.S. domain at 12 km resolution, and an East Texas domain at 4 km resolution as shown in Figure 3-1.

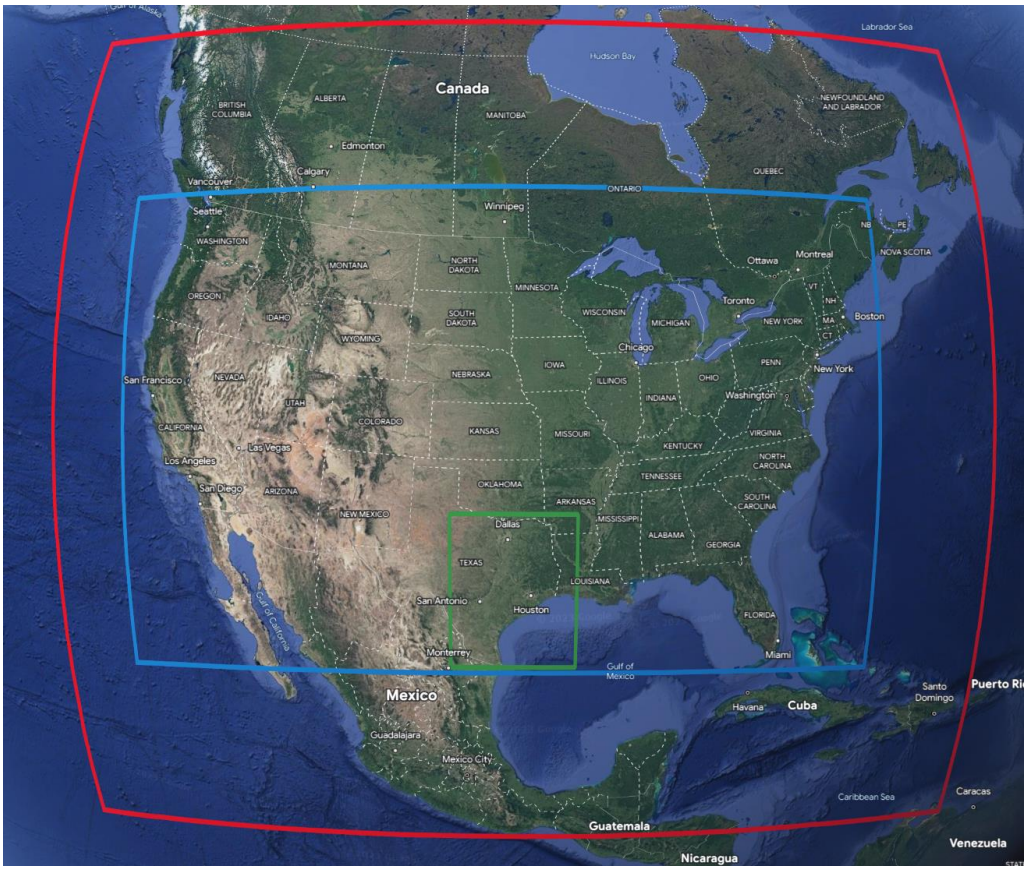

Figure 3-1. Nested grid domains in the TCEQ 2019 modeling platform.

For this project, TCEQ provided the following 2019 and 2023 modeling platform datasets:

- CAMx-ready gridded and point anthropogenic and biogenic emission input files for all grids;
- CAMx-ready meteorological input files for all grids derived using the Weather Research and Forecasting model (WRF; Skamarock et al., 2021);
- CAMx-ready ancillary input files (initial/boundary/top conditions, photolysis rates, ozone column map).

The TCEQ also provided example model configuration files and scripts to facilitate Ramboll's model setup. Table 3-1 lists the CAMx model configuration that was used for both 2019 and 2023.

Table 3-1. CAMx model configuration for TCEQ 2019 and 2023 modeling platform.

Model Options/Settings	CAMx Configuration
Version	v7.20
Date Range	March 16 – October 1 (Including March 16-31 spin-up period)
Time Zone	Central Standard Time (CST)
Map Projection	Lambert Conic Conformal
2-Way Nested Grid System	36/12/4 km (East Texas) horizontal grid resolution, 30 vertical layers up to ~20 km
Horizontal Advection	PPM
Vertical Advection	IMPLICIT
Gas-Phase Chemistry	CB6r5
Particulate Chemistry	CF2
Chemistry Solver	EBI
Dry Deposition	ZHANG03
Plume-in-Grid	Off
Bi-directional Ammonia	Off
Wet Deposition	On
ACM2 Boundary Layer Diffusion	Off
Surface Chemistry Model	Off
Inline Ix Emissions	On
Super Stepping	On
3-D Output	Off

The FEI processor's temporal allocation schemes distribute daily fire emissions to hourly emissions using a defined diurnal profile. There are currently two options in the FEI processor: 1) default: constant diurnal profile for all landcover types and 2) RAVE landcover: applies landcover-specific diurnal profiles developed from 5-minute FRP measurements by the RAVE team[2]. Because the RAVE product contains hourly emissions, the temporal allocation step is bypassed for the RAVE FEI.

The vertical allocation step in the FEI processor defines the top of the smoke plume (injection height) using one of two options: 1) PBL500 adds 500 m to the PBL height; or 2) Sofiev that uses a modified version of the injection height parameterization defined in Sofiev et al. (2012) that depends on FRP, PBL height and meteorological stability parameters. GFAS1.2 includes daily FRP, which we allocate to

[2] https://sites.google.com/view/rave-emission/diurnal-cycles?authuser=1

hourly FRP using the landcover-dependent FRP diurnal profiles developed by the RAVE team[3]. Because the RAVE product includes hourly FRP, we use this hourly FRP directly in the calculation of plume injection height in the Sofiev scheme.

Table 3-2 shows the FEI, temporal allocation and vertical allocation scheme selected for each CAMx simulation. Ramboll (2023) found that CAMx ozone and $PM_{2.5}$ concentrations in Texas were nearly identical when comparing sensitivity simulations that used the alternate temporal (default) and vertical (PBL500) allocation schemes. We chose the RAVE landcover and Sofiev schemes given better support in the scientific literature.

Table 3-2. FEI configuration options for each CAMx run conducted and evaluated.

CAMx Run	FEI Input	Temporal Scheme	Vertical Scheme
2019.run1	GFAS1.2	RAVE landcover	Sofiev
2023.run1	GFAS1.2	RAVE landcover	Sofiev
2023.run2	RAVE2.0	N/A (RAVE has hourly emissions)	Sofiev

3.2 2019 Model Performance Evaluation

This section presents the model performance evaluation for the 2019 CAMx modeling platform by comparing modeled results against observed data from monitoring sites within the TCEQ Continuous Ambient Monitoring Stations (CAMS) network. Table 3-3 summarizes the list of CAMS included in the 2019 analysis, along with the availability of ozone and $PM_{2.5}$ observations at each location. We evaluated model performance by analyzing the modeled maximum daily average 8-hour (MDA8) ozone statistics within each of the Dallas/Fort Worth (4 sites), Houston (4 sites) and San Antonio (3 sites) ozone nonattainment areas (NAA). Overall, the model demonstrated good ozone performance across all regions; detailed evaluation results are presented in the following sections. Figure 3-2 presents the monthly model performance statistics for MDA8 ozone during the April–September 2019 ozone season. The left panel shows the Normalized Mean Bias (NMB; %) and the right panel shows the Normalized Mean Error (NME; %), both computed using ozone observations from all CAMS monitors across the TCEQ 4 km domain. The orange bars show TCEQ's 2019 modeling results[4] (which used FINN2.2 fire emissions) and the blue bars show results from the 2019 GFAS simulation. The 2019 GFAS simulation exhibited smaller MDA8 ozone bias and error for each of the six months, with the largest discrepancies (better GFAS performance) found in April, May and September. This result is consistent with our previous 2019 evaluation (Ramboll, 2023), where GFAS outperformed FINN during April and May of 2019, when smoke transport from biomass burning in Mexico and Central America was frequent.

The 2019 modeling platform has an incomplete PM emissions inventory. We therefore cannot conduct a complete model evaluation for $PM_{2.5}$ and instead focused on hourly $PM_{2.5}$ time series, which we will provide at the conclusion of this project.

[3] https://sites.google.com/view/rave-emission/diurnal-cycles?authuser=1

[4] https://www.tceq.texas.gov/airquality/airmod/data/tx2019/stats_bar

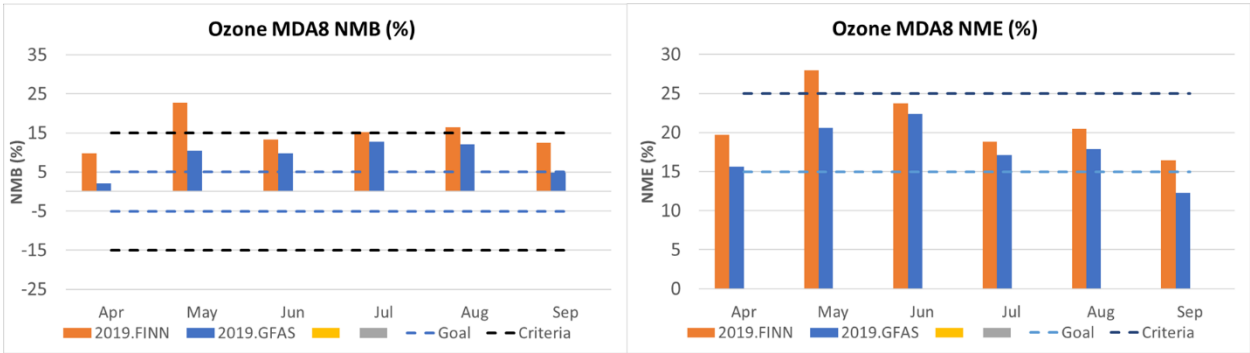

Figure 3-2. MDA8 ozone monthly NMB (%) and NME (%) bar plots for all Texas CAMS sites evaluated for TCEQ 2019 FINN (orange) and GFAS (blue) along with Goal (blue dashed) and Criteria (black dashed) performance benchmarks from Emery et al. (2017).

Table 3-3. Monitoring sites from the CAMS network for 2019 model performance evaluation.

Site Long Name/Info	CAMS Site ID	EPA AQS Site ID	Model Code	NAA	O3	PM
Frisco	31	480850005	FRIC	DFW	TRUE	FALSE
Dallas Hinton	401	481130069	DHIC	DFW	TRUE	TRUE
Dallas North No.2	63	481130075	DALN	DFW	TRUE	FALSE
Cleburne Airport	77	482510003	CLEB	DFW	TRUE	FALSE
Conroe Relocated	78	483390078	CNR2	HGB	TRUE	TRUE
Houston Aldine	8	482010024	HALC	HGB	TRUE	TRUE
Houston Bayland Park	53	482010055	BAYP	HGB	TRUE	FALSE
Houston Deer Park #2	35	482011039	DRPK	HGB	TRUE	TRUE
Camp Bullis	58	480290052	BOER	SAN	TRUE	FALSE
San Antonio Northwest	23	480290032	SAWC	SAN	TRUE	TRUE
Calaveras Lake	59	480290059	CALA	SAN	TRUE	TRUE

3.2.1 MDA8 Ozone Statistics

Figure 3-3 presents the model performance statistics for MDA8 ozone during the April–September 2019 ozone season. Similar to Figure 3-2, the left panel shows the NMB (%) and the right panel shows the NME (%). In this plot, statistics were computed using ozone observations from all CAMS monitors (as in Figure 3-2) and averaged over each of the major metropolitan areas: Dallas/Fort Worth (DFW), San Antonio (SAN), and Houston–Galveston–Brazoria (HGB; Houston hereafter). Each plot shows metrics for each month and for the entire 6-month period spanning April through September. The model achieves the Criteria benchmark performance metrics (±15% for NMB, <25% for NME; Emery et al., 2017) across most months and regions.

The Dallas–Fort Worth results exhibited the best agreement with observations, with NMB values remaining within the Goal benchmark for NMB (±5%) in each of the six months. San Antonio results showed larger biases but remained within the Criteria benchmark for NMB (±15%) for all months

except May (NMB: +18.4%). Houston results demonstrated the highest positive bias among the three regions, with NMB values surpassing the Criteria NMB benchmark in both July and August. Overall, the model demonstrated acceptable agreement with observations, with most values well within the Criteria metrics (±15% for NMB, 25% for NME).

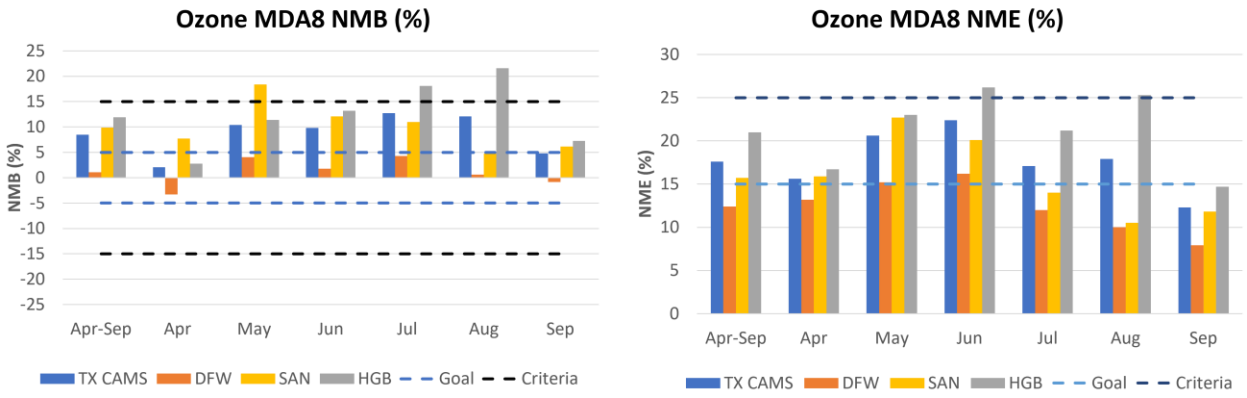

Figure 3-3. MDA8 ozone April-September and monthly NMB (%) and NME (%) bar plots for all Texas CAMS sites evaluated here (blue), Dallas/Fort Worth CAMS (orange), San Antonio CAMS (yellow) and Houston CAMS (gray) along with Goal (blue dashed) and Criteria (black dashed) performance benchmarks.

Accompanying this report are detailed statistics tables for each CAMS in Table 3-3. Also accompanying this report are interactive, zoomable HTML map overlays showing episode and monthly average NMB and NME statistics for all CAMS in Table 3-3. We omitted these tables and maps in this report for brevity, but we concluded from these products that the 2019 GFAS run performed well.

3.2.2 MDA8 Ozone Time Series

Accompanying this report are time series plots of observed and modeled MDA8 ozone concentrations at the CAMS listed in Table 3-3. Figure 3-4 shows an example MDA8 ozone time series plot at Frisco C31. Observations are shown as black dotted lines, while CAMx 2019.run1 (GFAS) outputs are depicted in solid red. In general, the time series showed that the model successfully simulated most of the highest ozone events and the model aligned well with the observed daily variability in ozone levels during most of the modeling period. Further, we found no substantial differences between CAMS within the same region.

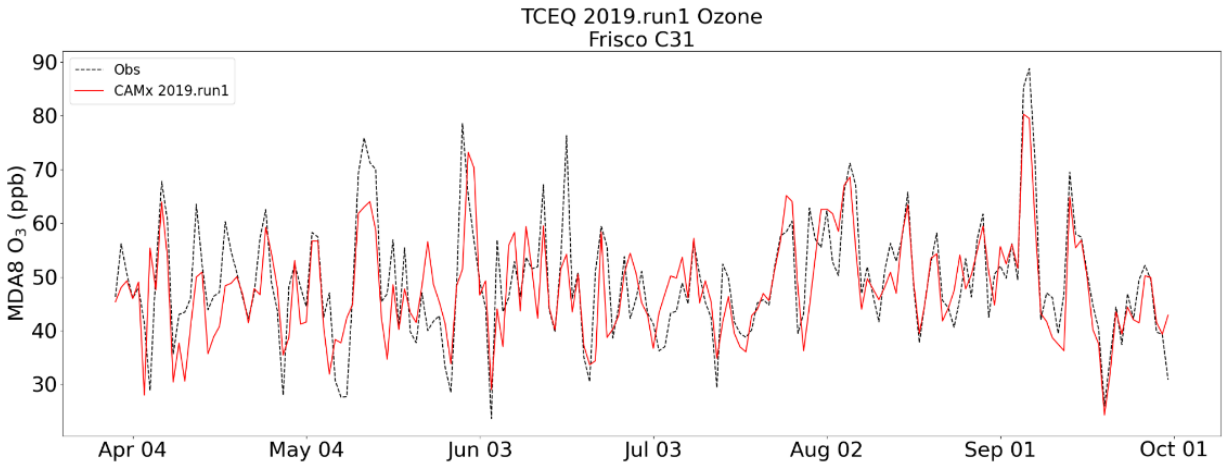

Figure 3-4. Time series of modeled and observed MDA8 O3 at Frisco C31.

3.3 2023 Model Performance Evaluation

Table 3-4 summarizes the list of CAMS included in the 2023 model performance evaluation, along with the availability of ozone and $PM_{2.5}$ observations at each location. We evaluated the model performance by analyzing the modeled MDA8 ozone statistics within each of four CAMS in the Dallas/Fort Worth region, three CAMS in Houston, and three CAMS in San Antonio. Overall, the model demonstrated good ozone performance across all regions for both the GFAS1.2 and RAVE2.0 runs. We recommend RAVE2.0 due to superior ozone agreement with observations during the high observed ozone period in August and September of 2023. Detailed evaluation results are presented in the following sections.

As with the 2019 modeling platform, the 2023 platform has an incomplete PM emissions inventory. We therefore cannot conduct a complete model evaluation for FEI impacts on $PM_{2.5}$ and instead provide hourly $PM_{2.5}$ time series at the conclusion of this project.

Table 3-4. Monitoring sites from the CAMS network for the 2023 model performance evaluation.

Site Long Name/Info	CAMS Site ID	EPA AQS Site ID	Model Code	NAA	O3	PM
Pilot Point	1032	481211032	PIPT	DFW	TRUE	FALSE
Frisco	31	480850005	FRIC	DFW	TRUE	FALSE
Cleburne Airport	77	482510003	CLEB	DFW	TRUE	FALSE
Ft. Worth Northwest	13	484391002	FWMC	DFW	TRUE	TRUE
Houston Bayland Park	53	482010055	BAYP	HGB	TRUE	TRUE
Houston East	1	482011034	HOEA	HGB	TRUE	TRUE
Galveston 99th St.	1034	481671034	GALV	HGB	TRUE	TRUE
Camp Bullis	58	480290052	BOER	SAN	TRUE	FALSE
San Antonio Northwest	23	480290032	SAWC	SAN	TRUE	TRUE
Calaveras Lake	59	480290059	CALA	SAN	TRUE	TRUE

3.3.1 MDA8 Ozone Statistics

Figure 3-5 presents the model performance statistics for MDA8 ozone during the April–September 2023 modeling period. The top panel shows NMB and the bottom panel shows NME, both computed using ozone observations from all Texas CAMS in Table 3-4 and averaged over the CAMS in each area: Dallas/Forth Worth (DFW), San Antonio (SAN), and Houston (HGB). Statistics are shown for each month and the April–September 6-month modeling period.

Both the GFAS1.2 (2023.run1; shown in blue) and RAVE2.0 (2023.run2; shown in orange) runs exhibit similar patterns of NMB and NME across months and regions. RAVE2.0 ozone concentrations are generally higher, resulting in larger overpredictions and smaller underpredictions compared to GFAS1.2. The most pronounced bias occurs in April, with both runs overpredicting ozone across all regions. Notably, San Antonio exceeds the Criteria benchmark in April and June. During the high observed ozone period of August and September 2023, RAVE2.0 demonstrates smaller bias than GFAS1.2, indicating improved performance in capturing peak ozone levels.

In terms of error, both runs display similar NME patterns across months and regions, with the largest errors occurring in April, when transport of smoke from fires in Mexico and Central America was frequent (Ramboll, 2023). GFAS1.2 shows slightly smaller error than RAVE2.0 in April and generally maintains lower error from April through July. In contrast, RAVE2.0 outperforms GFAS1.2 with lower error in August and September, further supporting its stronger performance during this high ozone period.

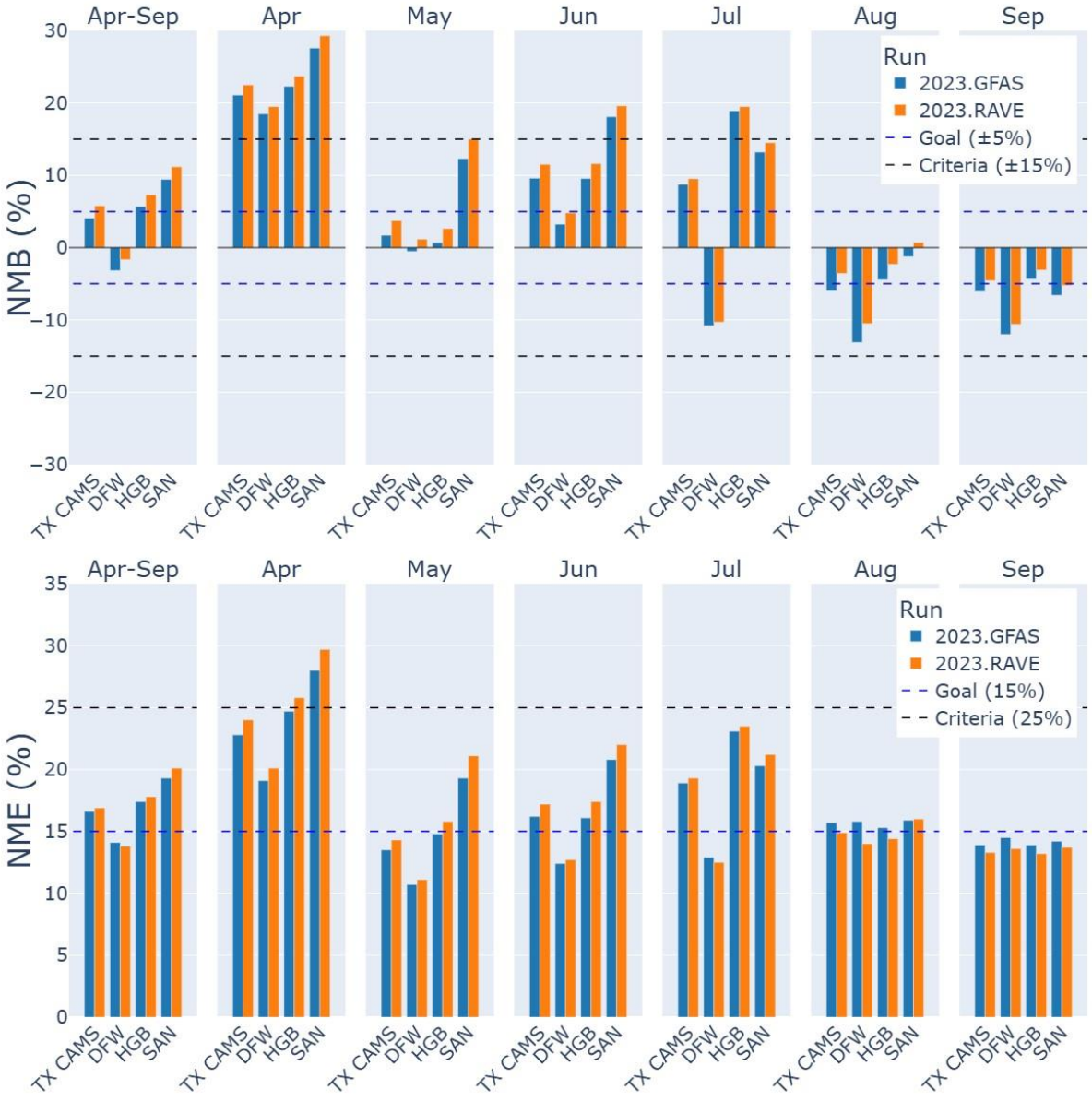

Figure 3-5. MDA8 ozone monthly average NMB (%; top) and NME (%; bottom) bar plots over all Texas CAMS sites addressed in this analysis, Dallas/Fort Worth, Houston, and San Antonio regions. 2023.run1 (GFAS) results are shown in blue and 2023.run2 (RAVE2.0) results are shown in orange, along with Goal (blue) and Criteria (black) benchmarks shown as dashed lines.

Figure 3-6 shows the monthly average site-specific MDA8 ozone NMB on top and NME on the bottom for the Dallas/Fort Worth CAMS shown in Table 3-4, with results from 2023.run1 (GFAS) shown in blue and 2023.run2 (RAVE2.0) shown in orange. Both runs showed similar biases across months and sites: the RAVE2.0 run showed an overall smaller bias at all DFW sites and for all months except for April. The smallest biases occurred in May and June for both runs. During the high observed ozone period in August and September, the RAVE2.0 run exhibited notably smaller bias than GFAS. In terms of NME, both runs also showed similar patterns across most months and sites and the smallest errors occurred in May and June. However, the largest difference in error between the runs appeared in August, where RAVE2.0 demonstrated notably lower error. Overall, RAVE2.0 consistently showed lower error than GFAS during the high ozone period in August and September.

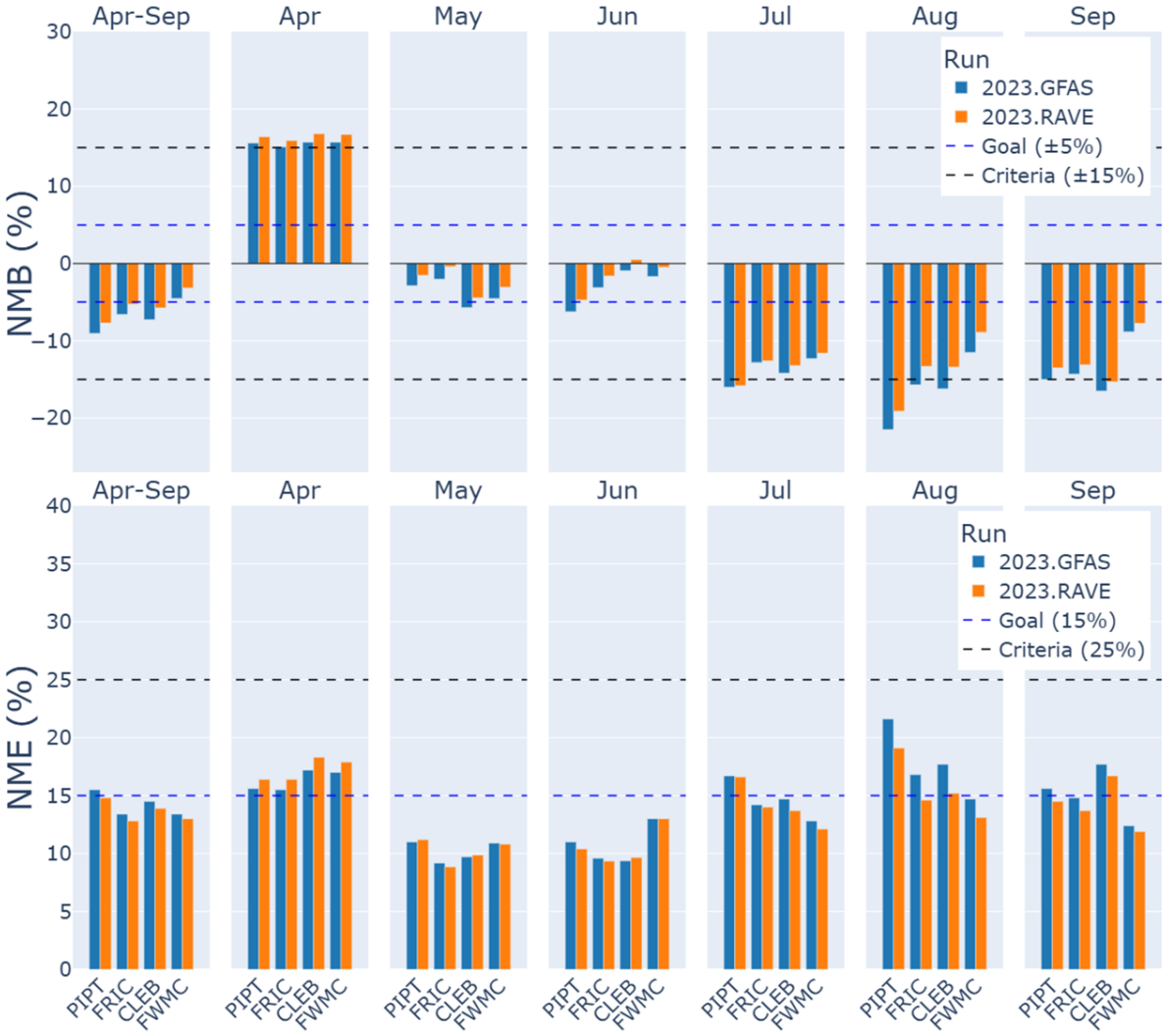

Figure 3-6. Site-specific MDA8 ozone monthly average NMB (%; top) and NME (%; bottom) bar plots for key CAMS sites in Dallas/Fort Worth region. 2023.run1 (GFAS) results are shown in blue and 2023.run2 (RAVE2.0) results are shown in orange, along with Goal (blue) and Criteria (black) benchmark shown as dashed lines.

Figure 3-7 shows the monthly average site-specific MDA8 ozone NMB (top) and NME (bottom) for key CAMS in Houston. GFAS results are shown in blue and RAVE2.0 results are shown in orange. Both runs exhibited similar biases across months and sites, with the notable variation among individual sites. The near-zero bias observed over the full April–September period resulted from the offsetting effects of positive and negative monthly biases. During the high observed ozone period in August and September, the RAVE2.0 run showed notably smaller biases compared to GFAS. Similarly, both runs displayed comparable error patterns across months and sites. The Houston CAMS generally met the Goal benchmark for NME throughout the modeling period, though substantial variability existed across months and locations. RAVE2.0 also demonstrated lower error than GFAS during the high ozone months.

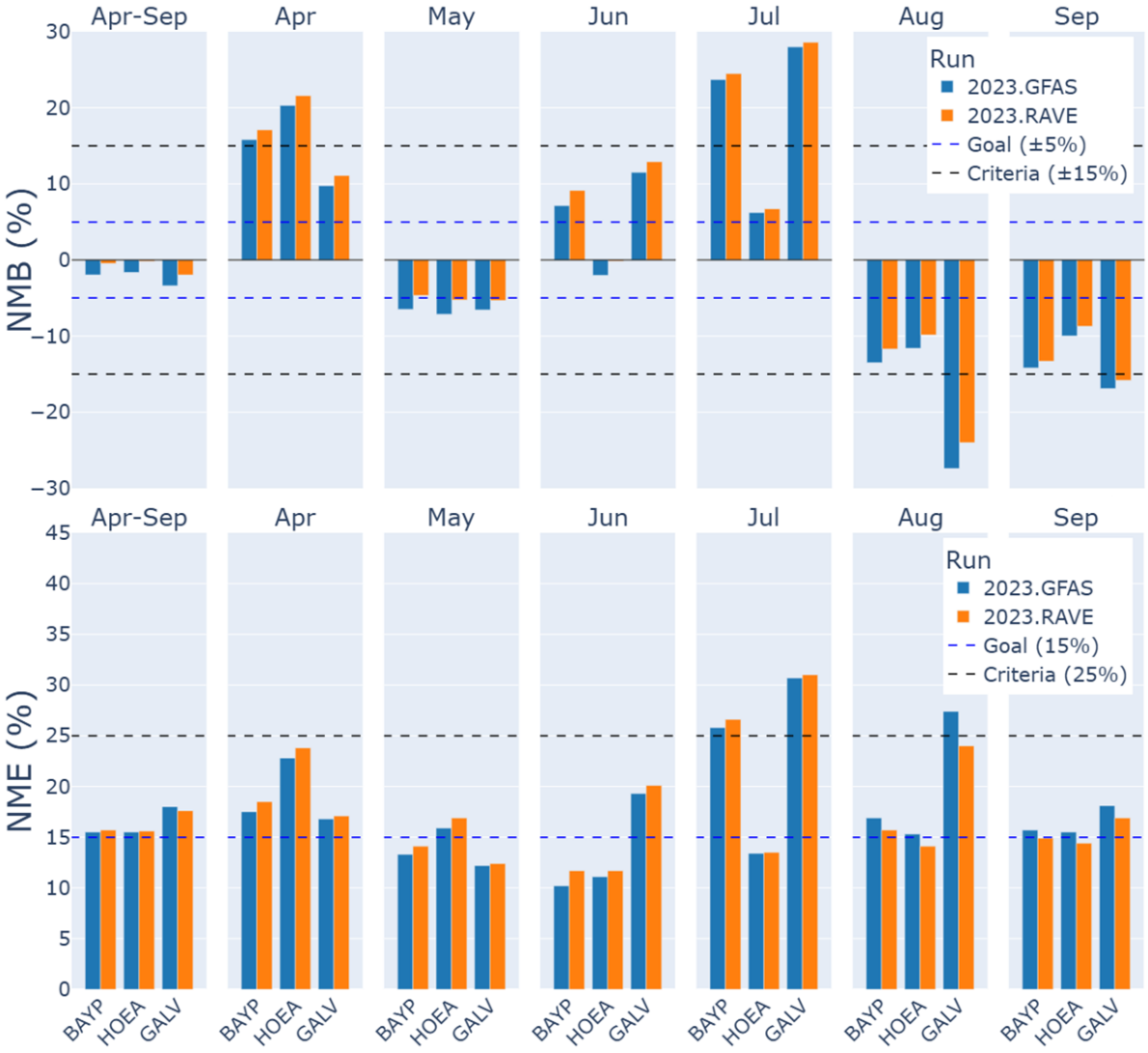

Figure 3-7. Site-specific MDA8 ozone monthly average NMB (%; top) and NME (%; bottom) bar plots for key CAMS sites in Houston. 2023.run1 (GFAS) results are shown in blue and 2023.run2 (RAVE2.0) results are shown in orange, along with Goal (blue) and Criteria (black) benchmark shown as dashed lines.

Figure 3-8 shows the monthly average site-specific MDA8 ozone NMB (top) and NME (bottom) for key CAMS in San Antonio. GFAS results are shown in blue and RAVE2.0 results are shown in orange. Both runs exhibited similar biases across months and sites in the region, with some variation observed among individual sites. The near-zero bias over the April–September period average reflected the cancellation of positive and negative monthly biases. During the high observed ozone period in August and September, the RAVE2.0 run showed smaller bias than GFAS. Similarly, both runs displayed comparable error patterns across months and sites, and San Antonio sites remained within the Goal benchmark for the April–September period. RAVE2.0 also demonstrated lower error than GFAS during the August–September high ozone period.

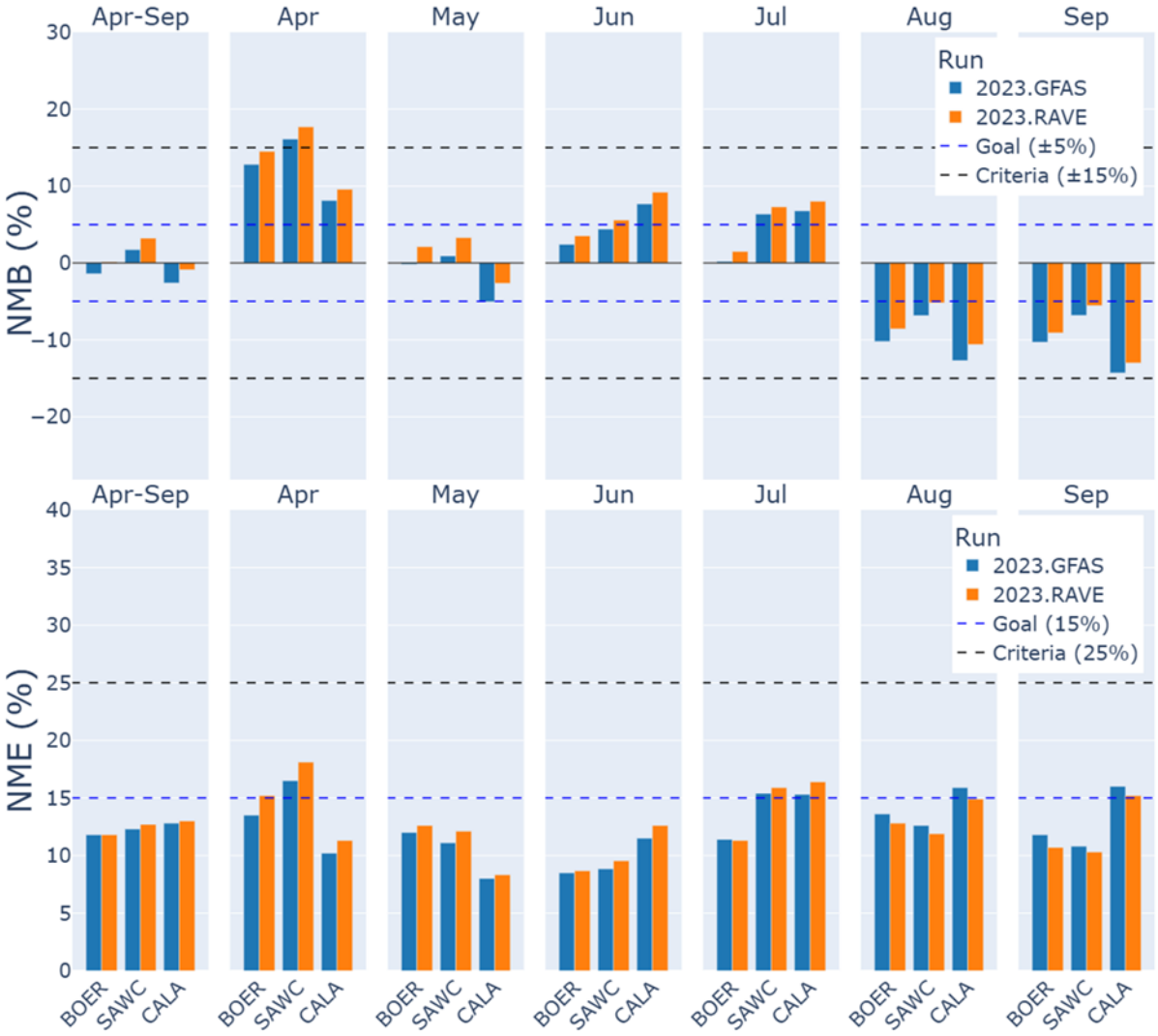

Figure 3-8. Site-specific MDA8 Ozone monthly average NMB (%; top) and NME (%; bottom) bar plots for key CAMS sites in San Antonio. 2023.run1 (GFAS) results are shown in blue and 2023.run2 (RAVE2.0) results are shown in orange, along with Goal (blue) and Criteria (black) benchmark shown as dashed lines.

3.3.2 MDA8 Ozone Time Series

Figure 3-9 shows time series comparisons of observed and modeled MDA8 ozone concentrations at four Dallas/Fort Worth CAMS, with GFAS1.2 results shown in red and RAVE2.0 results shown in blue. Both runs demonstrated reasonable ability to capture the temporal trends and seasonal patterns of observed ozone concentrations across all sites, with modeled concentrations generally falling within the 30-80 ppb range observed in the measurements. The models demonstrated adequate performance during moderate ozone periods but showed consistent underprediction of peak ozone episodes, particularly during the high ozone season from mid-July through September when observed values frequently exceeded 80-90 ppb. RAVE2.0 showed better performance compared to GFAS1.2 across most sites, with better representation of elevated ozone events during high ozone periods. Site-specific differences were evident, and Pilot Point C1032 and Frisco C31 sites displayed the largest discrepancies between modeled and observed peak concentrations.

Figure 3-10 shows similar time series for three Houston CAMS. Both GFAS1.2 and RAVE2.0 runs demonstrated good agreement with observed temporal patterns and seasonal variability across all Houston sites. Both runs effectively captured the transition from high ozone periods in late spring through mid-June, the subsequent mid-summer minimum during late June and July, and the high ozone period from August through September. The models showed particularly strong performance during the May-June high ozone episodes, and both runs tracked observed peaks that frequently exceeded 80 ppb at Houston Bayland Park C53 and Houston East C1. During the mid-summer low ozone period from July through early August, both runs maintained close alignment with the observed concentrations. RAVE2.0 exhibited marginally better performance compared to GFAS1.2 across most sites and time periods, with notably better representation of peak events during the September ozone season at all three locations. Site-specific differences were noticeable: Galveston 99th Street C1034 showed the most consistent model-observation agreement throughout the simulation period, and Houston Bayland Park C53 and Houston East C1 sites displayed occasional underpredictions during extreme ozone events.

Figure 3-11 shows similar time series for three San Antonio CAMS. Both GFAS1.2 and RAVE2.0 runs demonstrated good agreement with observed temporal patterns and seasonal variability across all sites, and both runs effectively captured the spring ozone buildup from April through June, the mid-summer decline through July followed by elevated concentrations during the mid-August through September. The models showed particularly strong performance during moderate ozone periods, and both runs tracked observed concentrations that typically ranged from 30-70 ppb across all three sites. Both GFAS1.2 and RAVE2.0 exhibited similar performance characteristics throughout most of the simulation period, with close alignment during the high ozone episodes in May-June and September. Site-specific differences were minimal, with Camp Bullis C58 and San Antonio Northwest C23 showing nearly identical model-observation agreement patterns. Each model run showed consistent underprediction of peak episodes at all three CAMS, particularly during the high ozone season from mid-August through September. RAVE2.0 exhibited marginally better performance at capturing peak ozone concentrations during high ozone episodes in August and September.

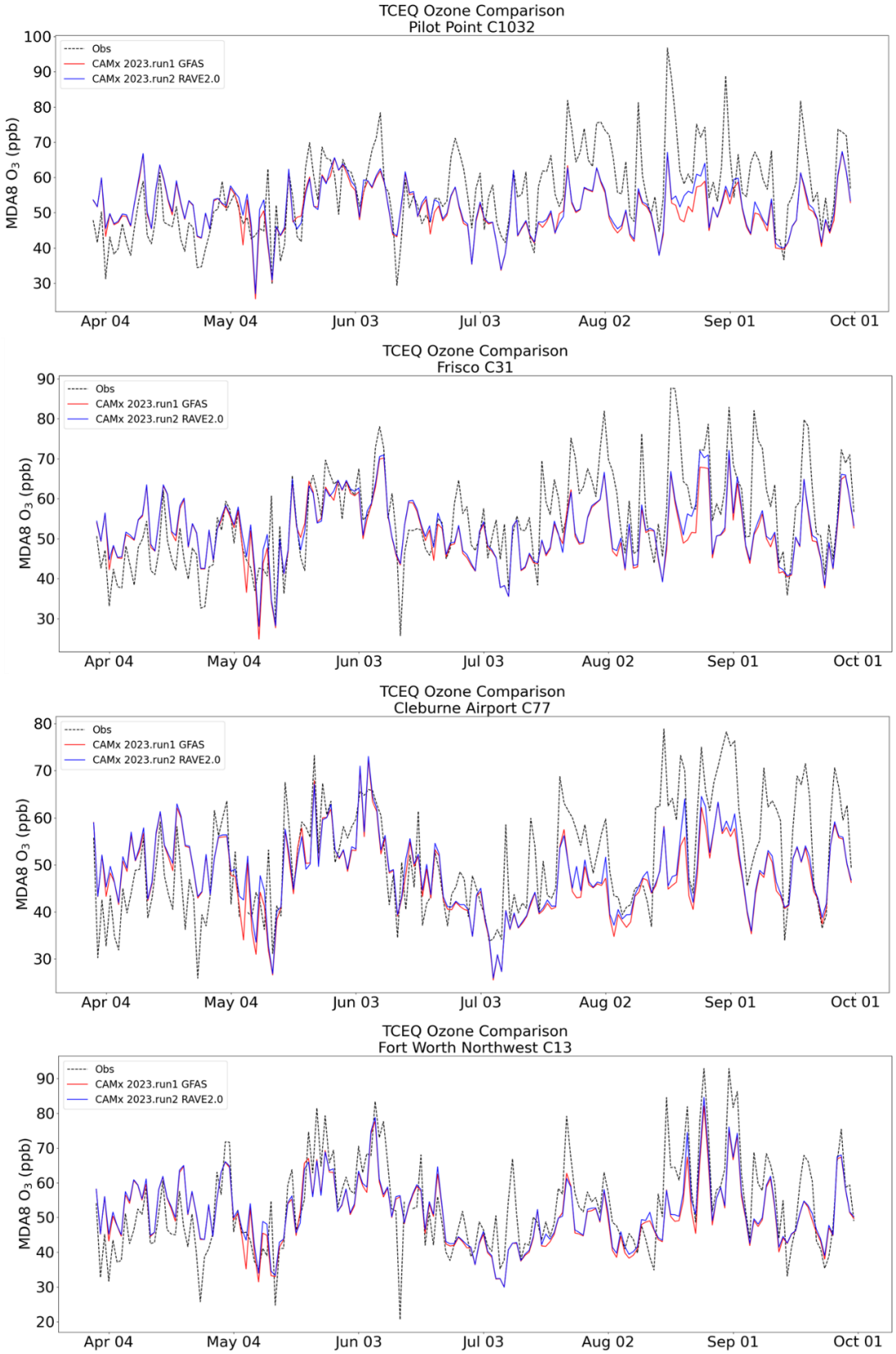

Figure 3-9. Time series of modeled and observed MDA8 O3 at Dallas/Fort Worth Sites (from top to bottom: Pilot Point C1032, Frisco C31, Cleburne Airport C77, and Fort Worth Northwest C13).

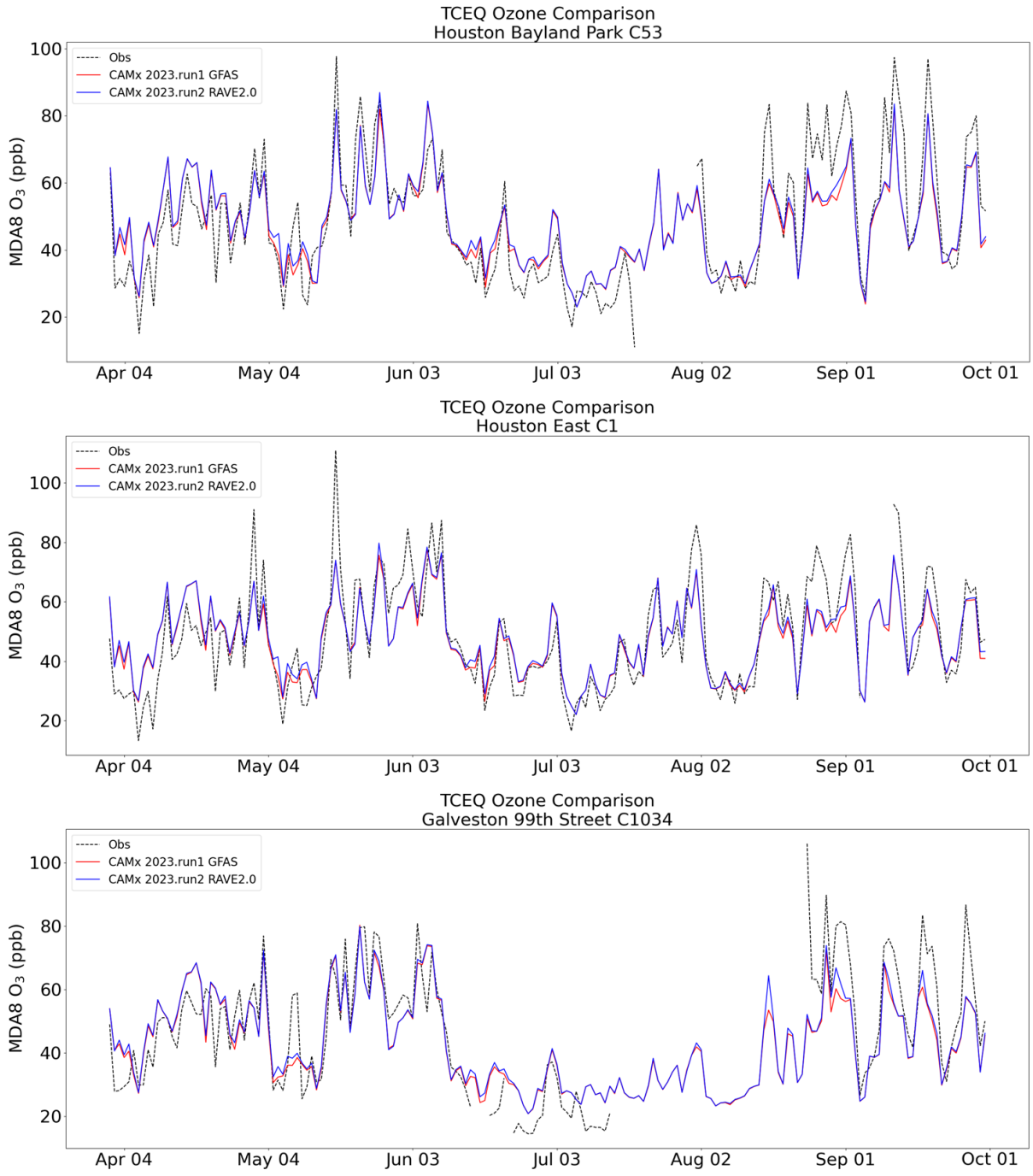

Figure 3-10. Time series of modeled and observed MDA8 ozone at Houston CAMS (from top to bottom: Bayland Park C53, Houston East C1, and Galveston 99th Street C1034).

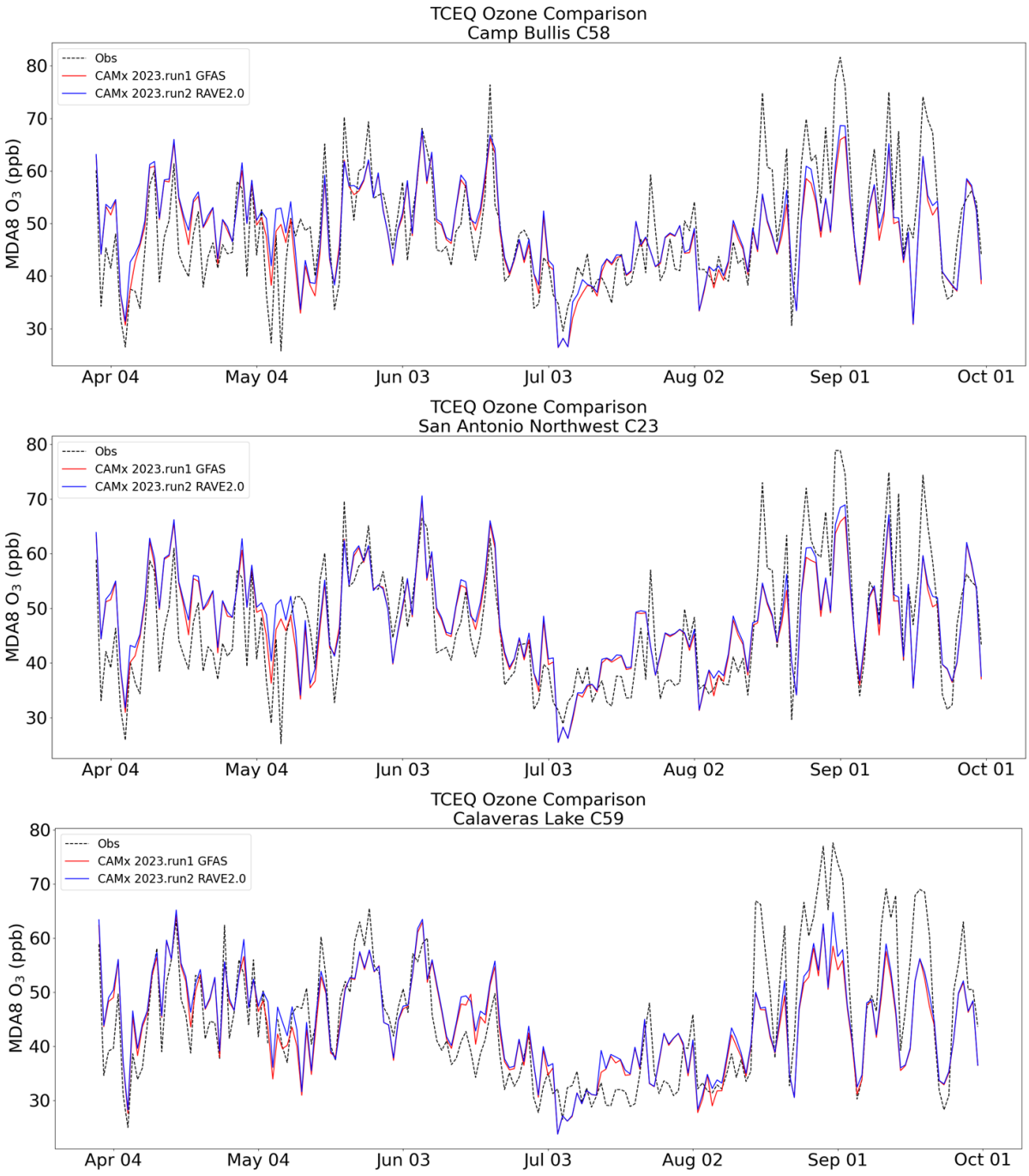

Figure 3-11. Time series of modeled and observed MDA8 ozone at San Antonio CAMS (from top to bottom: Camp Bullis C58, San Antonio Northwest C23, and Calaveras Lake C59).

4.0 CONCLUSIONS AND RECOMMENDATIONS

In the first phase of this project, Ramboll developed model-ready fire emissions for April-September of 2019 and 2023 using Ramboll's FEI processor. This processor, originally developed in 2022 (Ramboll, 2022), can generate model-ready fire emissions from five different FEIs.

Ramboll (2023) found that the GFAS1.2 FEI showed substantially smaller modeled ozone biases and overall better statistical agreement with observations compared to FINN2.2, which was used in TCEQ's 2019 modeling. All modeling was conducted using CAMx (Ramboll, 2024b).

Like other FEIs, GFAS1.2 has daily temporal and 0.1° spatial resolution. A newer FEI, RAVE2.0, offers finer temporal (hourly) and spatial (0.03°) resolution. Ramboll (2024a) found RAVE2.0 resulted in the best overall model agreement with ozone and $PM_{2.5}$ observations among all available FEIs in a CAMx application for the active Summer 2021 wildfire season in the Western U.S. Since RAVE2.0 fire emissions are only available from 2021 onward, we developed GFAS1.2 fire emissions for the April-September 2019 CAMx modeling application and developed both GFAS1.2 and RAVE2.0 emissions for the 2023 application. Both years used TCEQ's CAMx modeling platforms. We could not perform CAMx modeling and evaluation for 2022 because TCEQ's 2022 modeling platform was not ready in time for this project.

Our evaluation of the 2019 GFAS1.2 CAMx simulation shows good ozone performance across all regions, with lower monthly bias and error than TCEQ's 2019 modeling, which used FINN2.2 fire emissions. This result aligns with our more extensive testing of four different FEIs for the shorter April-May 2019 period (Ramboll, 2023). The ozone evaluation for the 2023 CAMx simulations found similar results between GFAS1.2 and RAVE2.0. GFAS1.2 exhibited slightly better performance during April-May, while RAVE2.0 performed slightly better during August-September, when observed ozone was highest. We recommend RAVE2.0 for 2023 due to its superior ozone performance during the highest ozone periods.

Ramboll recommends three activities to improve the FEI processor and support TCEQ's needs:

- Complete model performance evaluation for 2022 and provide recommendations for choice of FEI
- Use CAMx to evaluate FEI processor updates that use fire intensity rather than fuel type for VOC speciation
- Develop model-ready fire emissions for 2024 using multiple FEIs and conduct CAMx simulations and ozone and $PM_{2.5}$ evaluation

5.0 REFERENCES

Emery, C., Liu, Z., Russell, A.G., Odman, M.T., Yarwood, G. and Kumar, N., 2017. Recommendations on statistics and benchmarks to assess photochemical model performance. Journal of the Air & Waste Management Association, 67(5), pp.582-598.

Li, F., X. Zhang, S. Kondragunta, X. Lu, I. Csiszar, C. C. Schmidt. 2022. Hourly biomass burning emissions product from blended geostationary and polar-orbiting satellites for air quality forecasting applications. Remote Sensing of Environment. https://doi.org/10.1016/j.rse.2022.113237.

Ramboll. 2022. Develop Tools to Process and Evaluate Options for Improved Fire Emission Inventories. Ramboll US Consulting, Inc., Novato CA. Prepared for the Texas Commission on Environmental Quality. June 2022.

Ramboll, 2023. Fire Emission Inventory Processing. Prepared for the Texas Commission on Environmental Quality. June 2023.

Ramboll, 2024a. Fire Emission Inventory Development for 2022 Modeling Platform. Prepared for the Texas Commission on Environmental Quality. June 2024.

Ramboll, 2024b. User's Guide – Comprehensive Air Quality Model with Extensions Version 7.30. Available at www.camx.com. August 2024.

Rémy, S., Veira, A., Paugam, R., Sofiev, M., Kaiser, J. W., Marenco, F., Burton, S. P., Benedetti, A., Engelen, R. J., Ferrare, R., and Hair, J. W. 2017. Two global data sets of daily fire emission injection heights since 2003, Atmos. Chem. Phys., 17, 2921–2942, https://doi.org/10.5194/acp-17-2921-2017.

Skamarock, W. C., Klemp, J. B., Dudhia, J., Gill, D. O., Liu, Z., Berner, J., Wang, W., Powers, J. G., Duda, M. G., Barker, D., Huang, X.Y. 2021. A Description of the Advanced Research WRF Model Version 4.3 (No. NCAR/TN-556+STR). Doi:10.5065/1dfh-6p97

Sofiev, M., Ermakova, T., & Vankevich, R. 2012. Evaluation of the smoke-injection height from wild-land fires using remote-sensing data. Atmospheric Chemistry and Physics, 12(4), 1995–2006. https://doi.org/10.5194/acp-12-1995-2012